Soluble monomeric acetylcholinesterase from mouse: Expression, purification, and crystallization in complex with fasciculin

PASCALE MARCHOT,[1,6] RAIMOND B.G. RAVELLI,[2] MIA L. RAVES,[3,5] YVES BOURNE,[1,4,7] DANIEL C. VELLOM,[1,8] JOAN KANTER,[1] SHELLEY CAMP,[1] JOEL L. SUSSMAN,[3,5] AND PALMER TAYLOR[1]

[1] Department of Pharmacology, University of California at San Diego, La Jolla, California 92093-0636
[2] Department of Crystal and Structural Chemistry, Bijvoet Center for Biomolecular Research, Padualaan 8, 3584 CH Utrecht, The Netherlands
[3] Biology Department, Brookhaven National Laboratory, Upton, New York 11973
[4] Department of Molecular Biology, The Scripps Research Institute, La Jolla, California 92037
[5] Department of Structural Biology, Weizmann Institute of Science, Rehovot 76100, Israel

Abstract

A soluble, monomeric form of acetylcholinesterase from mouse (mAChE), truncated at its carboxyl-terminal end, was generated from a cDNA encoding the glycophospholipid-linked form of the mouse enzyme by insertion of an early stop codon at position 549. Insertion of the cDNA behind a cytomegalovirus promoter and selection by aminoglycoside resistance in transfected HEK cells yielded clones secreting large quantities of mAChE into the medium. The enzyme sediments as a soluble monomer at 4.8 S. High levels of expression coupled with a one-step purification by affinity chromatography have allowed us to undertake a crystallographic study of the fasciculin-mAChE complex. Complexes of two distinct fasciculins, Fas1-mAChE and Fas2-mAChE, were formed prior to the crystallization and were characterized thoroughly. Single hexagonal crystals, up to 0.6 mm × 0.5 mm × 0.5 mm, grew spontaneously from ammonium sulfate solutions buffered in the pH 7.0 range. They were found by electrophoretic migration to consist entirely of the complex and diffracted to 2.8 Å resolution. Analysis of initial X-ray data collected on Fas2-mAChE crystals identified the space group as $P6_122$ or $P6_522$ with unit cell dimensions $a = b = 75.5$ Å, $c = 556$ Å, giving a V_m value of 3.1 Å^3/Da (or 60% of solvent), consistent with a single molecule of Fas2-AChE complex (72 kDa) per asymmetric unit. The complex Fas1-mAChE crystallizes in the same space group with identical cell dimensions.

Keywords: acetylcholinesterase; crystallization; fasciculin; peptide–macromolecule complex; snake toxin

Reprint requests to: Palmer Taylor, Department of Pharmacology, University of California at San Diego, La Jolla, California 92093-0636.

[6] Permanent address: Laboratoire de Biochimie, CNRS, Unité de Recherche Associée 1455, Institut Fédératif de Recherche Jean Roche, Université d'Aix-Marseille II, Faculté de Médecine Secteur Nord, 13916 Marseille cedex 20, France.

[7] Permanent address: Laboratoire de Cristallisation et Cristallographie des Macromolécules Biologiques, CNRS, Institut Fédératif de Recherche Concertée-1, 31 Ch. Joseph Aiguier, 13402 Marseille cedex 20, France.

[8] Present address: Department of Biochemistry, Brooklyn College of the City University of New York, Brooklyn, New York 11210-2889.

Acetylcholinesterase's only well-documented action is the termination of receptor activation by the neurotransmitter, acetylcholine, at synaptic junctions through ester hydrolysis (cf. Massoulié et al., 1993; Taylor & Radić, 1994). Inhibition of acetylcholinesterase gives rise to a panoply of symptoms. In skeletal muscle, fasciculations are observed initially, followed by flaccid paralysis.

Fasciculins are the only known peptide inhibitors of AChE, with dissociation constants as low as 1–10 pM. These 7-kDa peptides, which are found in mamba snake venoms (cf. Cerveñansky et al., 1991), form three loops emerging from a dense core containing the disulfide bridges. They belong to the structural family of three-fingered peptidic toxins from Elapidae venoms, which include the nicotinic receptor-blocking α-neurotoxins (Changeux et al., 1970; Endo & Tamiya, 1991), the muscarinic receptor peptide agonists (Adem et al., 1988; Segalas et al., 1995), and the

cardiotoxins that interact with cell membranes (Bougis et al., 1981; Dufton & Hider, 1991). Despite a common structural motif, the toxins in this family are directed to diverse targets, yet their modes of action are highly selective. Several lines of evidence show that the fasciculins bind to a peripheral site of AChE, a region distinct from the catalytic center and located at the rim of the active site gorge. This site shares a common region with the binding site, of peripheral-site cationic inhibitors and with the site at which the substrate, when present in large excess, binds. In addition, fasciculins appear not to totally occlude access of small molecules to the catalytic site (Marchot et al., 1993; Radić et al., 1995). Rather, they influence AChE catalysis in an allosteric fashion, although a partial gating influence may also restrict the rate of entry into the gorge for substrates whose catalysis is rate-limited or near-limited by diffusion (Eastman et al., 1995; Radić et al., 1995; van den Born et al., 1995).
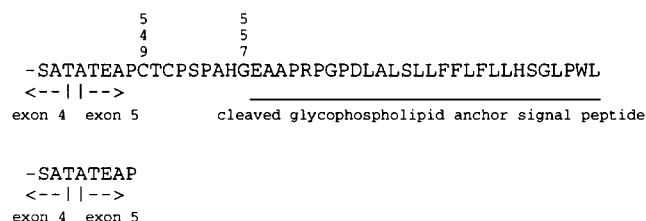
The X-ray structure of a dimeric AChE from *Torpedo californica* has been solved at 2.8 Å resolution (Sussman et al., 1991). Since then, substantial information regarding the fasciculin binding site on mouse AChE has been obtained by site-directed mutagenesis (Radić et al., 1994, 1995). The X-ray structures of fasciculins, Fas1 and Fas2, have been solved at 1.9 Å and 2.0 Å resolution, respectively (Le Du et al., 1992, 1995). Analysis of the structures, however, allowed one only to hypothesize on the nature of the fasciculin determinants responsible for binding to AChE.

The predominant monomeric and dimeric forms of native AChE contain a hydrophobic domain at their carboxyl-terminus, either as an attached glycophospholipid or an amphipathic sequence (Massoulié et al., 1993), both being likely to limit the propensity for crystallization. In the dimeric *Torpedo* AChE, the diglyceride on the glycophospholipid, which serves as the hydrophobic anchor in the membrane, was enzymatically cleaved prior to crystallization (Sussman et al., 1988).

We have generated a soluble, monomeric AChE from mouse (mAChE), a catalytic subunit (~65 kDa), from a cDNA lacking the coding sequence for the extreme carboxyl terminus. High levels of expression in HEK cells, coupled with a one-step purification by affinity chromatography on an inhibitor-conjugated resin, have allowed us to undertake an X-ray crystallographic study of the fasciculin–AChE complex.

Results and discussion

Insertion of a stop codon in place of the Cys 549 codon of mouse AChE (Rachinsky et al., 1990; Li et al., 1991, 1993) maintains the catalytic core of the molecule, but truncates 37 amino acids from the nascent peptide. This eliminates the signal for attachment of the hydrophobic glycophospholipid to the carboxy-terminal residue (Gly 557) of the processed native enzyme (Fig. 1). Thus, the recombinant DNA-derived enzyme is nine residues shorter than the processed amphiphilic enzyme and, importantly, lacks a hydrophobic glycophospholipid or amphipathic helix at its carboxyl-terminus found on other forms of AChE. HEK cells in which the mutated cDNA was stably integrated were grown in the presence of serum, then allowed to express mAChE in a serum-free medium. Typically, 0.2–0.5 mg of mAChE was secreted over a 3-day period in a 10-cm dish covered with 10 mL of medium, and secretion at a high level could

```
          5         5
          4         5
          9         7
-SATATEAPCTCPSPAHGEAAPRPGPDLALSLLFFLFLLHSGLPWL
<-- | | -->
exon 4  exon 5         cleaved glycophospholipid anchor signal peptide


-SATATEAP
<-- | | -->
exon 4  exon 5
```

Fig. 1. Carboxyl-terminal sequences of native and truncated mouse AChE. The signal for attachment of the hydrophobic glycophospholipid to Gly 557 in the processed native enzyme (top sequence) has been eliminated by insertion of a stop codon in place of the Cys 549 codon. The resulting enzyme, mAChE, is monomeric and devoid of a carboxyl-terminal hydrophobic segment (bottom sequence). Sequence Ser-Ala-Thr is encoded by the end of exon 4; sequence Ala-Thr-Glu is encoded by the beginning of exon 5 (Li et al., 1993). Mouse AChE residue numbering is used.

be maintained for up to one month. Sedimentation of mAChE from the collected medium on sucrose gradients in the presence of 1% Triton X-100 yielded a single, symmetric peak sedimenting at 4.8 S (Fig. 2), consistent with the recombinant enzyme sedimenting as a monomer. Indeed, dimers of the catalytic subunit containing the glycophospholipid sediment at 6.0 S, whereas cleavage of the phospholipid yields a sedimentation constant of 6.5 S (D.C. Vellom, unpubl. data). Similar behavior has been reported for corresponding forms of *Torpedo* AChE (Duval et al., 1992).

Purification and characterization of mAChE

Similar to the procedure adopted for purification of the 11S form of *T. californica* AChE (Taylor & Jacobs, 1974), affinity chromatography was used to purify milligram quantities of mAChE from the tissue culture medium. Typically, 30–50 mg of enzyme in 2–4 L of medium were subjected to purification by selective retention on an *m*-aminophenyltrimethyl-ammonium-
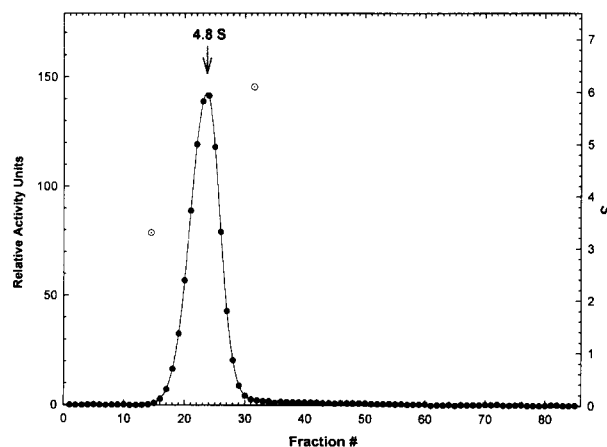

Fig. 2. Hydrodynamic analysis of mAChE-containing harvested culture media. The sample (100 μL), supplemented with sedimentation standards, was centrifuged in a 3–20% sucrose gradient in the presence of Triton X-100, then fractionated as described in the text. Sedimentation positions of two standards, carbonic anhydrase (3.3 S) and alkaline phosphatase (6.1 S), are shown as dotted open circles.

conjugated column and subsequent elution by decamethonium. Owing to the high concentration of decamethonium used, mAChE eluted as a single, sharp peak with only minor tailing representing a few percent of the initial activity loaded on the column. Purification yields ranged from 60% to 95% of the activity initially detected in the medium. The specific activity of purified mAChE, 2,206 units mg^{-1}, corresponds to a k_{cat} of 16.2×10^4 min^{-1}, in good agreement with the value reported previously (Vellom et al., 1993). Routine storage at $-20\,°C$ of purified mAChE mixed with glycerol 1:1 (v/v) was not consistent with reliable crystallization. An immediate and dramatic loss of activity was observed upon flash-freezing of the purified enzyme in liquid nitrogen. mAChE, however, could be stored for weeks on ice without loss of activity or alteration of the gel-filtration or SDS-PAGE patterns.

Electrophoretic analysis of the purified mAChE suggests that the enzyme displays slight heterogeneity. Indeed, SDS-PAGE resulted in two diffuse and partially overlapping bands with a ratio of about 1:1 and an average apparent mass of ca. 65 kDa (Figs. 3, 4A), whereas native gel electrophoresis resulted in a diffuse and particularly broad band, larger than expected from a protein with three *N*-glycosylation sites (Fig. 4B). Reducing the volume of the loaded sample and/or increasing the crosslinking of the stacking gel did not change these patterns significantly. Removal of the N-linked carbohydrate side chains from mAChE by digestion with PNGaseF, then subsequent analysis by SDS-PAGE, resulted in sharpening of the two bands, causing them to migrate closer to each other, and lowering their apparent mass to ca. 55 kDa (Fig. 3). The purified mAChE could therefore be composed of two roughly equal populations of monomeric en-

Fig. 3. Electrophoretic analysis of native and deglycosylated mAChE. SDS-PAGE (15% resolving/5% stacking gel, 20 cm × 20 cm) under reducing conditions: lanes 1 and 6, purified mAChE; lanes 2 and 7, BSA (66 kDa); lanes 3 and 4, mAChE deglycosylated with PNGaseF; lane 5, BSA treated with PNGaseF. The thin band at the bottom of the gel corresponds to PNGaseF (36 kDa, lanes 3, 4, and 5).
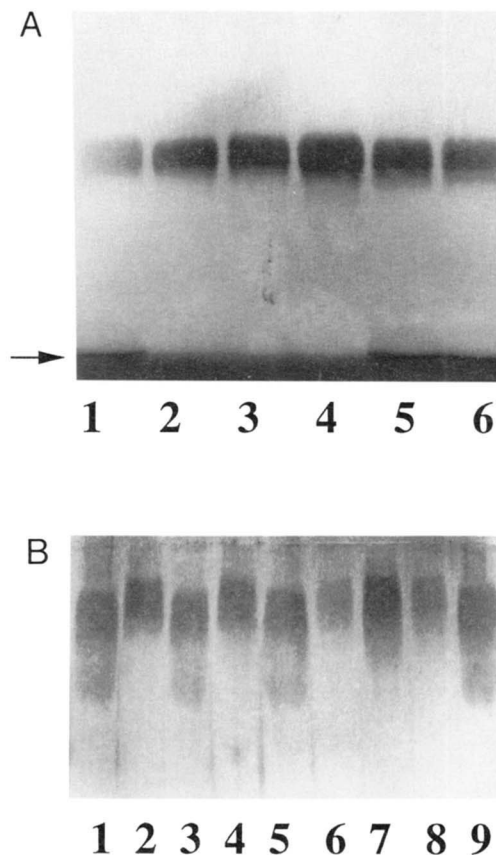
Fig. 4. Electrophoretic analysis of mAChE and fasciculin–mAChE complexes. **A:** SDS-PAGE (4–20% gradient gel, 8 cm × 8 cm) under reducing conditions: lanes 2, 3, and 4, purified mAChE; lane 1, mAChE complexed to Fas1; lane 5, mAChE complexed to Fas2; lane 6, washed and dissolved Fas2-mAChE hexagonal crystal; mAChE migrates as two diffuse and overlapping bands; arrow at the bottom of the gel indicates the fasciculin band (lanes 1, 5, and 6). **B:** Native gel electrophoresis (7.5% resolving/5% stacking gel, 8 cm × 8 cm) with migration toward the anode: lanes 1, 3, 5, and 9, purified mAChE; lane 2, mAChE complexed to Fas1; lane 4, mAChE complexed to Fas2; lanes 6, 7, and 8, washed and dissolved triangular, needle-shaped, and hexagonal Fas2-mAChE crystals, grown in (NH$_4$)$_2$SO$_4$; the shift toward the cathode in the position of the complexes (lanes 2, 4, 6, 7, and 8) relative to the free mAChE is evident.

zyme differing slightly in their carbohydrate composition or some other post-translational modification. Similar observations have been reported for purified recombinant human AChE (Velan et al., 1992). Independent analysis of the chromatographic fractions from the affinity column showed that the two bands co-elute throughout the elution peak, suggesting identical binding properties for the two forms. The two forms were still observed upon SDS-PAGE analysis of the fasciculin–mAChE complexes and of the dissolved crystals (Fig. 4; see below), and therefore are not distinguished by complexation with fasciculin and subsequent crystallization.

Complexation of mAChE with fasciculins and characterization of the complexes

Special care has been taken for complexation of Fas1 and Fas2, respectively, to mAChE and characterization of the complexes

prior to crystallization. The fasciculin–mAChE complexes were preformed at, or close to, the high protein concentrations required for crystallization, i.e., a concentration ~10^8-fold greater than the K_i of Fas2 for mouse AChE (Radić et al., 1994), together with an 1.2 molar excess of fasciculin. Slightly higher residual activity was observed repeatedly for the Fas2-mAChE complex compared to the Fas1-mAChE complex. Both complexes were analyzed by gel electrophoresis (after removal of the unbound excess fasciculin) and gel filtration chromatography (before and after removal). SDS-PAGE of the complexes was performed with a gradient gel appropriate for the large difference in size of the fasciculin and the mAChE molecules (Fig. 4A). Although fasciculin migrated together with the free dodecyl-sulfate, it ran as a thin, intense band at the bottom of the gel. The migration pattern of initially complexed mAChE was found to be identical to free mAChE. In order to establish actual complexation of Fas1 or Fas2 to mAChE and not only their simultaneous presence, native gel electrophoresis was performed both on the free and complexed mAChE (Fig. 4B). The bound fasciculin was found to diminish the mobility of mAChE, as expected from the increased Mw or/and basicity of the complex compared to the free enzyme. Identical electrophoretic patterns were observed for the Fas1- and Fas2-mAChE complexes.

Gel filtration chromatography of the free mAChE and the fasciculin–mAChE complexes led to single, symmetric absorbance peaks (data not shown). No difference in the chromatographic mobility of the fasciculin–mAChE complexes with regard to mAChE could be detected, most probably because of the limited resolution for a mass change from ~65 kDa to ~72 kDa. Screening the chromatographic fractions for their AChE activity, however, required 10^3-fold less dilution of the fasciculin–mAChE fractions than the mAChE fractions, consistent with the level of residual activity (in the 0.1% range) recorded upon complexation of mAChE. Screening for fasciculin activity of the fractions eluting from chromatography of the fasciculin–mAChE complexes performed *before* removal of the unbound fasciculin revealed an included free fasciculin peak eluting at a position consistent with its mass. No such fasciculin peak was detected upon equivalent screening of the fractions eluting from chromatography of the fasciculin–mAChE complexes performed *after* removal of the unbound fasciculin, thereby affirming the total removal of the excess fasciculin.

Crystallization of the fasciculin–mAChE complexes

Crystals spontaneously grew within 2–5 days in hanging drops and within a week in sitting drops. Various crystal morphologies were obtained in two major conditions based on the use of PEG or $(NH_4)_2SO_4$ as precipitating agents. Thick needles with hexagonal sections, extending across the droplet and sometimes hollowed at one end, grew similarly from PEG 600, 2000, 4000, or 10000 solutions buffered with 0.1 M NaAc or ImMal at pHs between 6.5 and 7.5. In contrast, three different crystal forms were obtained from 1.25 M to 1.45 M $(NH_4)_2SO_4$, buffered to pH 6.5 to 7.5 with ammonia. Short and large needles with hexagonal sections, thick triangles, stars, and crowns, all made of stacked thin triangular platelets, as well as symmetric hexagons with slightly variable geometry, were generally found in the same drop, although with varying distribution depending on the precise $(NH_4)_2SO_4$ concentration or pH (Fig. 5A,B). Growth of hexagonal needles as perpendicular axes from the triangles or
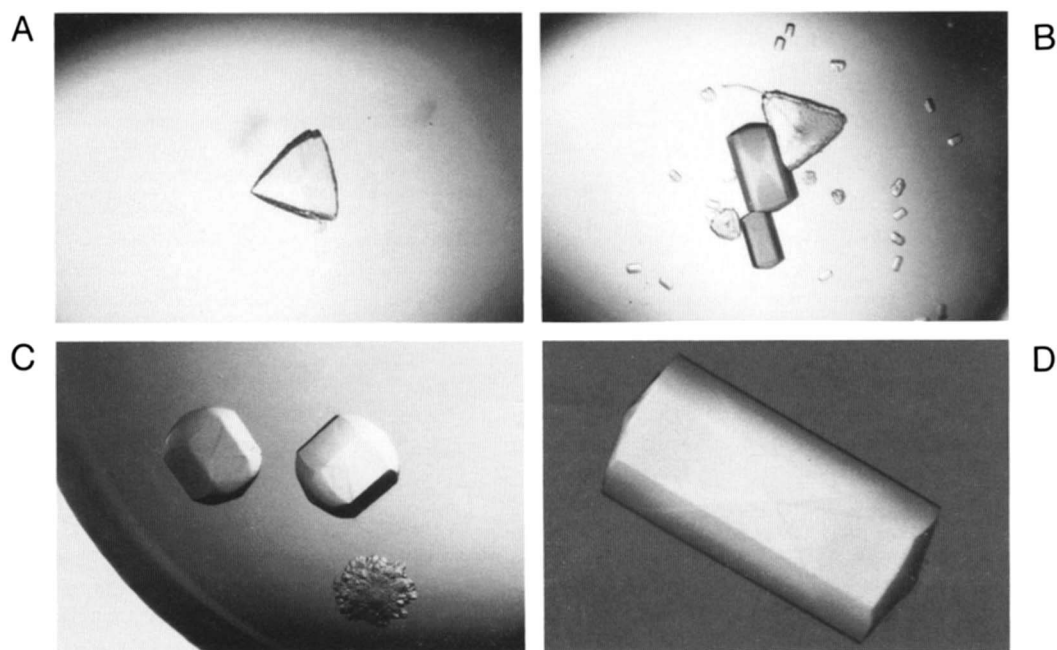
Fig. 5. Photographs of fasciculin-mAChE crystals. **A,B:** Fas1-mAChE and Fas2-mAChE crystals spontaneously grown in a 4-μL hanging drop from 1.35 M $(NH_4)_2SO_4$, pH 6.75. **C:** Half Fas2-mAChE crystals (0.6 mm × 0.5 mm × 0.25 mm) spontaneously grown in a 10-μL sitting drop from 1.35 M $(NH_4)_2SO_4$, pH 7.25. **D:** Fas2-mAChE crystal (1 mm × 0.5 mm × 0.5 mm) grown from 1.35 M $(NH_4)_2SO_4$, pH 7.0, by macroseeding of a 10-μL drop.

as parallel axes from the hexagons was sometimes observed, suggesting that the three forms crystallize in related, if not identical, space groups. Buffering the $(NH_4)_2SO_4$ solutions with 0.1 M NaAc, ImMal, or $NaKPO_4$, as well as adding 0.25% (w/v) β-octylglucoside, did not change the crystallization behavior significantly. Triangular crystals could not be dissociated to monocrystals, even when grown in the presence of 0.25% or 0.5% (w/v) β-octylglucoside or 0.1% (w/v) heptanediol or the detergent screening kit solutions. Growing the hexagonal Fas2-AChE crystals in sitting drops occasionally led to half-crystals adhering tightly to the siliconized cover-slip, presumably arising from epitaxial nucleation (Fig. 5C).

Except for the hexagonal form, which grew almost specifically from the Fas2-mAChE complex (only three hexagonal Fas1-mAChE crystals were obtained in a unique drop after ~10 weeks of equilibration), the same crystal forms were obtained for the two complexes. They all could be enlarged by macroseeding. Larger hexagonal Fas2-mAChE crystals were so obtained (Fig. 5D). Cross-seeding of the Fas1-mAChE complex with seeds from a hexagonal Fas2-mAChE crystal led to both triangular and hexagonal Fas1-mAChE crystals, although the latter grew more slowly than their Fas2 counterparts and displayed a slightly different geometry (not shown). The two fasciculins differ by a single substitution Fas1-Tyr to Fas2-Asn at position 47. No difference, however, could be found in their affinity for mAChE (P. Marchot, unpubl. data). Differences in solubility of the two complexes should therefore account for their different crystallization behavior. The protein content of all crystal forms was checked by SDS-PAGE and native-gel electrophoresis after several successive rinses of the crystals in decreasing concentrations of the precipitating agent, then dissolution in distilled water (Fig. 4A,B). In all cases, the patterns were the same as observed initially upon analysis of the complexes in solution, indicating actual crystallization of the fasciculin-mAChE complexes rather than mAChE alone. Free mAChE, even when concentrated to 18–20 mg mL^{-1}, remained totally soluble in all conditions that yielded fasciculin-mAChE crystals.

Data collection

Preliminary X-ray studies were performed at beam line X12B of the National Synchrotron Light Source (NSLS) equipped with a standard MarResearch imaging plate detector. The highest diffracting patterns (2.8 Å) were obtained for the hexagonal Fas2-mAChE crystals as compared to triangles (3.5 Å) and PEG- or $(NH_4)_2SO_4$-grown needles (5 Å) from both complexes, but the diffraction limit dropped to about 4 Å after the first 15° rotation of data collection. With the aim of protecting the crystals from radiation damage, numerous cryoprotection and flash-cooling assays were performed, but all failed because of immediate cracking of the crystal or/and dramatic loss of resolution. Preliminary data were therefore collected at 4 °C. The crystals belong to space group $P6_122$ or $P6_522$ with cell dimensions $a = b = 75.5$ Å, $c = 556$ Å, giving a V_m value of 3.1 Å^3/Da or 60% of solvent, consistent with the presence of a single molecule of complex (72 kDa) in the asymmetric unit (Matthews, 1968). Efforts to collect data at beam line X12B, however, were hampered by the large dimension of the c axis and the resulting overlap of the diffraction spots. Diffraction data were therefore collected at beam line X12C of the NSLS, equipped with a Mar-

Research imaging plate detector mounted on an Enraf Nonius 4-circle goniometer. A distance of 540 mm ($\lambda = 1.5$ Å) and 860 mm ($\lambda = 1.0$ Å) with a tilt of 11° and 12°, respectively, was used with 2° oscillation steps. A total of ca. 62,200 observations was obtained at 3.2 Å from four Fas2-mAChE crystals, giving ca. 14,500 unique reflections (85% complete, $R_{sym} = 8.9\%$). Further details on the crystallographic parameters of the Fas2-mAChE complex have been presented elsewhere (Bourne et al., 1995).

The same resolution limit was observed for the spontaneously grown hexagonal Fas1-mAChE crystals, which belong to the same space group with similar cell dimensions $a = b = 75.4$ Å, $c = 550$ Å. In spite of the apparently different conformations of their first disulfide loop, loop I (Le Du et al., 1992, 1995), Fas1 and Fas2 would be expected to adopt the same conformation upon binding to mAChE. The crystals, however, were most probably heterogeneous because double diffraction patterns were obtained. Diffraction patterns from triangles and needles were also consistent with a particularly long c axis.

In summary, the expression of a recombinant cDNA-derived form of AChE, truncated by nine amino acids from native mouse AChE, has yielded a monomeric enzyme appropriate for structural studies. The solubility of mAChE decreased in the presence of fasciculin, and crystals of fasciculin-mAChE complexes suitable for X-ray analysis have been obtained (Bourne et al., 1995). This structure offers a new template for further structure-function studies of mammalian cholinesterases. The structures of the fasciculin-AChE complexes (Bourne et al., 1995; Harel et al., 1995) contribute to at least three lines of investigation. First, they help reveal how fasciculin inhibits AChE. Second, they represent the first structures of three-fingered snake toxins bound to their macromolecular receptors. Third, establishing the contact points between fasciculin and AChE provides a framework for understanding the bases of the high affinities and unusual specificities of the family of three-fingered peptidic toxins.

Materials and methods

Materials

HEK-293 cells were obtained from American Type Culture Collection. Ultraculture cell culture medium was purchased from Biowhittaker. Dialysis tubing (Spectra/Por6) was from Spectrum Medical Industries. Centriprep, Centricon, and Microcon concentration units were from Amicon. Sterile 0.22-μm SpinX units were from Costar. The BCA kit for protein assays was from Pierce. The prepacked Superose-12 HR 10/30 column was from Pharmacia. Gel-filtration molecular weight markers (Mw-GF-70 Kit) were from Sigma. Precast Tris-glycine 4–20% gradient gels were from Novex. Prestained protein Mw standards for SDS-PAGE (14,300–200,000 Mw range) were from Gibco BRL. PNGaseF (S.A., 12,500,000 U mg^{-1}) was from BioLabs. DTNB, ATCh, decamethonium bromide, and PEG 200 were from Sigma. All other PEG (600, 2000, 4000, and 10000), as well as ammonium sulfate of biochemical grade, were from Fluka. The Detergent Screening Kit was from Hampton Research. All buffers used for crystallization were made with deionized water from a Millipore MilliRO/MilliQ system and filtered through 0.22-μm cellulose acetate membrane filtration units (Corning).

Proteins

Fas1 and Fas2 were from the same purification batches as those used previously for crystallization and structure determination (Le Du et al., 1989, 1992, 1995). The concentrations of stock solutions were determined from their UV spectra (ϵ_{276nm} = 6,300 M^{-1} cm^{-1} for Fas1 and 4,900 M^{-1} cm^{-1} for Fas2). mAChE was a soluble molecular form derived from the cDNA encoding the glycophospholipid-linked form of mouse AChE (Li et al., 1993). The cDNA was truncated after Pro 548 by insertion of a stop codon (TGA) in place of the Cys 549 codon (Fig. 1). Sequence of the mutant cDNA was confirmed by direct sequencing of the insert. The cDNA was inserted behind a CMV promoter. Transfection into HEK cells was with $Ca_3(PO_4)_2$ co-precipitation (Vellom et al., 1993). Selection of clones depended on incorporation of the neomycin-resistance gene and selection of cells with G418 sulfate (800 μg mL^{-1}) (Radić et al., 1993; Vellom et al., 1993). HEK-293 cells in which the mutated mAChE cDNA was stably integrated were grown to confluency in Dulbecco's modified Eagle's medium supplemented with 10% fetal bovine serum, then switched into serum-free media (Ultraculture) for collection of secreted mAChE.

Assay of AChE activity

AChE activity measurements were conducted spectrophotometrically (Ellman et al., 1961) with 0.5 mM acetylthiocholine iodide and 0.33 mM DTNB in 100 mM NaH_2PO_4/Na_2HPO_4, pH 7.0, BSA 0.1 mg mL^{-1}, to a final volume of 1.5 mL (room temperature). Initial kinetics of duplicate samples were recorded at λ = 412 nm during 5 min with a Response™ spectrophotometer (Gilford). A specific activity of 30,000 ΔA min^{-1} mg^{-1} was used. Relative AChE activities were screened at room temperature by microtitration on a Vmax kinetic microplate reader (Molecular Devices Corp.) with λ = 405 nm. Gel-filtration fractions were diluted 20–50,000-fold for screening of free mAChE and 30-fold for screening of the residual activity of the fasciculin-AChE complexes. Free fasciculin in the chromatographic fractions was screened by recording the residual activity of an extra AChE sample (~8 pM) after incubation for 1 h at 37 °C with a 30–100-fold dilution of the fractions (Marchot et al., 1993).

Sedimentation velocity analysis

mAChE-containing culture medium was sedimented into linear 3–20% sucrose gradients containing 0.1 M NaCl, 0.04 M $MgCl_2$, 0.01 M Tris-HCl, pH 8.0, and 0.1% (v/v) Triton X-100, for 20 h at 200,000 $\times$ g (4 °C). The layered sample (100 μL) was supplemented with carbonic anhydrase (20 μg, 3.3 S), alkaline phosphatase (0.2 μg, 6.1 S), catalase (2 μg, 11.4 S), and β-galactosidase (0.4 μg, 16 S) as sedimentation standards (Camp et al., 1995). The sedimented 12-mL tubes were fractionated in 96-tube racks with the microtitration plate format allowing further screening of the respective enzyme activities.

Purification and characterization of mAChE

Soluble mAChE was purified by affinity chromatography using *m*-trimethylaminophenyl amine coupled to Sepharose through a successively coupled succinic acid and diaminodipropylamine arm (Taylor & Jacobs, 1974). The conjugated resin was stored as a 50% suspension in 100 mM NaCl, 40 mM $MgCl_2$, 10 mM $NaHCO_3$, pH 8.0, containing NaN_3 0.02% (w/v). Harvested Ultraculture medium containing the expressed mAChE was centrifuged (2,000 g, 15 min, 4 °C) to remove cell debris, and assayed for AChE activity. $MgCl_2$ (1 M) was added to a final concentration of 40 mM, then the resin suspension (1 mL for each 2 mg AChE), and the mixture was allowed to stir in a spinner flask overnight at 4 °C in the presence of NaN_3 0.02% (w/v). The mixture was assayed for residual AChE activity and, if required, supplemented with the exact amount of resin necessary to achieve total inhibition of the enzyme. It was poured into a Bio-Rad econo column, allowed to pack by sedimentation, then washed with the equilibrating buffer (50–100-fold the bed volume). The bound AChE was eluted with 100 mM decamethonium bromide (30 $\times$ K_i, Radić et al. 1993) in the same buffer, at a low flow rate (1–1.5 mL h^{-1}). Elution fractions were assayed for AChE activity with a 10^6-fold final dilution, which reduced the final decamethonium concentration to well below its K_i for the mouse enzyme. The purified enzyme was dialyzed *extensively* against the crystallization buffer with SpectraPor6 dialysis tubing, then rinsed again and concentrated to 10–20 mg mL^{-1} in a Centriprep3 or Centricon3 unit. Purified mAChE was quantified independently from catalytic activity, BCA protein assay, absorbance at λ = 280 nm, and titration by Fas2 (Marchot et al., 1993), all of which yielded a close correlation. It was stored on ice.

N-linked carbohydrate removal

Purified mAChE (20 μg in 100 μL) was boiled for 10 min in denaturing buffer: 20 mM Tris-HCl, pH 8.0, 5 mM EDTA, 5 mM β-mercaptoethanol, 0.5% (w/v) SDS, cooled, added with 1% (v/v) Nonidet P-40, then incubated in the presence of PNGaseF (2,000 U) for 5 h at 37 °C. A further aliquot of 2,000 U was added after 2 h of incubation.

Complexation of mAChE with fasciculins and crystallization of the complexes

The respective complexes were formed in 50 mM NaCl, 1 mM Mes, pH 6.5, NaN_3 0.01% (w/v) (crystallization buffer) with a fasciculin-to-AChE molar ratio of 1.2:1 to preclude stoichiometric deficiency assuming a maximal 10% error in the quantification of protein and peptide. After equilibration overnight on ice, the complexes were assayed for residual AChE activity and free fasciculin, respectively. The enzyme was considered to be totally complexed to fasciculin when no decrease in its residual activity (usually 0.1–0.5% of the initial activity of the sample) was observed upon further addition of fasciculin and extended incubation, and when free fasciculin could be detected in the mixture through inhibition of a second AChE sample. Excess fasciculin was then dialyzed from the complexes with the crystallization buffer in a Centricon10 or Microcon10 concentrator, until no free fasciculin could be detected in both the filtrate and the sample. Total removal was confirmed by gel-filtration chromatography. The complexes were concentrated to 12–15 mg mL^{-1}, then filtered through a SpinX unit. They were stored on ice and were used within a week with no change in their crystallization behavior. Both Fas1- and Fas2-AChE complexes were crystal-

lized at 20 °C by the vapor diffusion method using hanging drops (4 µL) or sitting drops (10 µL) with a protein-to-well solution ratio of 1:1. Macroseeding of 10 µL sitting drops previously equilibrated overnight was performed according to Stura and Wilson (1992).

Electrophoresis

SDS-PAGE under reducing conditions and native gel electrophoreses of mAChE and Fas-AChE complexes were performed according to the discontinuous system of Laemmli (1970) with a vertical gel electrophoresis apparatus (JM Specialty Parts) or a Mighty Small Slab gel electrophoresis unit (Hoefer Scientific Instruments). Precast Tris-glycine 4–20% gradient gels, or 15% or 10% resolving/5% stacking gels, were used for SDS-PAGE. A 7.5% resolving/5% stacking gel made with no SDS was used for native gel electrophoresis. Samples loaded were typically 5 µL and contained 10% (v/v) glycerol. Silver nitrate staining was performed according to Morrisey (1981).

Gel-filtration chromatography

Analytical gel-filtration chromatography of mAChE and fasciculin–AChE complexes was conducted at 4 °C on a Superose-12 column using the FPLC system from Pharmacia. The column was equilibrated in, then eluted with, the crystallization buffer (flow rate, 0.5 mL min⁻¹). The loaded samples were 5 µL of the concentrated protein solutions used for complexation (mAChE) or crystallization (complexes), sandwiched into 25 µL of the crystallization buffer. Absorbance of column effluents was monitored at λ = 280 nm. Fractions (0.5 mL) were collected and assayed for AChE activity. The column was calibrated with a molecular weight standard kit.

Acknowledgments

References

Adem A, Asblom A, Johansson G, Mbugua PM, Karlsson E. 1988. Toxins from the venom of the green mamba *Dendroaspis angusticeps* that inhibit the binding of quinuclidinylbenzylate to muscarinic acetylcholine receptors. *Biochim Biophys Acta 968*:340–345.

Bougis P, Rochat H, Piéroni G, Verger R. 1981. Penetration of phospholipid monolayers by cardiotoxins. *Biochemistry 20*:4915–4920.

Bourne Y, Taylor P, Marchot P. 1995. Acetylcholinesterase inhibition by fasciculin: Crystal structure of the complex. *Cell 83*:503–512.

Camp S, Bon S, Li Y, Getman DK, Engel AG, Massoulié J, Taylor P. 1995. Patients with congenital myasthenia associated with end-plate acetylcholinesterase deficiency show normal sequence, mRNA splicing, and assembly of catalytic subunits. *J Clin Invest 95*:333–340.

Cerveñansky C, Dajas F, Harvey AL, Karlsson E. 1991. Fasciculins, anticholinesterase toxins from mamba venoms: Biochemistry and pharmacology. In: Harvey AL, ed. *Snake toxins*. New York: Pergamon Press Inc. pp 303–321.

Changeux JP, Kasai M, Lee CY. 1970. The use of a snake venom toxin to characterize the cholinergic receptor protein. *Proc Natl Acad Sci USA 67*:1241–1247.

Dufton MJ, Hider RC. 1991. The structure and pharmacology of elapid cytotoxins. In: Harvey AL, ed. *Snake toxins*. New York: Pergamon Press Inc. pp 259–302.

Duval NE, Krejci E, Grassi J, Coussen F, Massoulié J, Bon S. 1992. Molecular architecture of acetylcholinesterase collagen-tailed forms; construction of a glycolipid-tailed tetramer. *EMBO J 11*:3255–3261.

Eastman J, Wilson EJ, Cerveñansky C, Rosenberry TL. 1995. Fasciculin 2 binds to the peripheral site on acetylcholinesterase and inhibits substrate hydrolysis by slowing a step involving proton transfer during enzyme acylation. *J Biol Chem 270*:19694–19701.

Ellman GL, Courtney KD, Andres V Jr, Featherstone RM. 1961. A new rapid combination method for acetylcholinesterase activity. *Biochem Pharmacol 7*:88–95.

Endo T, Tamiya N. 1991. Structure–function relationship of postsynaptic neurotoxins from snake venoms. In: Harvey AL, ed. *Snake toxins*. New York: Pergamon Press Inc. pp 165–222.

Harel M, Kleywegt GJ, Ravelli RBG, Silman I, Sussman JL. 1995. Crystal structure of an acetylcholinesterase–fasciculin complex: Interaction of a three-fingered toxin from snake venom with its target. *Structure 3*: 1355–1366.

Laemmli UK. 1970. Cleavage of structural proteins during the assembly of the head of bacteriophage T4. *Nature (Lond) 227*:680–685.

Le Du MH, Housset D, Marchot P, Bougis PE, Navaza J, Fontecilla-Camps JC. 1996. Crystal structure of fasciculin 2 from mamba snake venom: Evidence for unusual loop flexibility. *Acta Crystallogr D52*:8.

Le Du MH, Marchot P, Bougis PE, Fontecilla-Camps JC. 1989. Crystals of fasciculin 2 from green mamba snake venom: Preparation and preliminary X-ray analysis. *J Biol Chem 264*:21401–21402.

Le Du MH, Marchot P, Bougis PE, Fontecilla-Camps JC. 1992. 1.9 Å resolution structure of fasciculin 1, an anti-cholinesterase toxin from green mamba snake venom. *J Biol Chem 267*:22122–22130.

Li Y, Camp S, Rachinsky TL, Getman D, Taylor P. 1991. Gene structure of mammalian acetylcholinesterase. *J Biol Chem 266*:23083–23090.

Li Y, Camp S, Taylor P. 1993. Tissue-specific expression and alternative mRNA processing of the mammalian acetylcholinesterase gene. *J Biol Chem 268*:5790–5797.

Marchot P, Khélif A, Ji YH, Mansuelle P, Bougis PE. 1993. Binding of ¹²⁵I-fasciculin to rat brain acetylcholinesterase. The complex still binds diisopropyl fluorophosphate. *J Biol Chem 268*:12458–12467.

Massoulié J, Pezzementi L, Bon S, Krejci E, Vallette FM. 1993. Molecular and cellular biology of the cholinesterases. *Prog Neurobiol 41*:31–91.

Matthews BW. 1968. Solvent content of protein crystals. *J Mol Biol 33*: 491–497.

Morrisey J. 1981. Silver stain for proteins in polyacrylamide gels; a modified procedure with enhanced uniform sensitivity. *Anal Biochem 117*:307–310.

Rachinsky TL, Camp S, Li Y, Ekström J, Newton M, Taylor P. 1990. Molecular cloning of mouse acetylcholinesterase: Tissue distribution of alternatively spliced mRNA species. *Neuron 5*:317–327.

Radić Z, Duran R, Vellom DC, Li Y, Cerveñansky C, Taylor P. 1994. Site of fasciculin interaction with acetylcholinesterase. *J Biol Chem 269*: 11233–11239.

Radić Z, Pickering NA, Vellom DC, Camp S, Taylor P. 1993. Three distinct domains in the cholinesterase molecule confer selectivity for acetyl- and butyrylcholinesterase inhibitors. *Biochemistry 32*:12074–12084.

Radić Z, Quinn DM, Vellom DC, Camp S, Taylor P. 1995. Allosteric control of acetylcholinesterase catalysis by fasciculin. *J Biol Chem 270*:20391–20399.

Segalas I, Roumestand C, Zinn-Justin S, Gilquin B, Ménez R, Ménez A, Toma F. 1995. Solution structure of a green mamba toxin that activates muscarinic acetylcholine receptors, as studied by nuclear magnetic resonance and molecular modeling. *Biochemistry 34*:1248–1260.

Stura E, Wilson IA. 1992. Seeding techniques. In: Ducruix A, Giege R, eds. *Crystallization of nucleic acids and proteins, a practical approach*. Oxford: IRL Press, Oxford University Press. pp 99–126.

Sussman JL, Harel M, Frolow F, Oefner C, Goldman A, Toker L, Silman I. 1991. Atomic structure of acetylcholinesterase from *Torpedo californica*: A prototypic acetylcholine-binding protein. *Science 253*:872–879.

Sussman JL, Harel M, Frolow F, Varon L, Toker L, Futerman AH, Silman I. 1988. Purification and crystallization of a dimeric form of acetylcholinesterase from *Torpedo californica* subsequent to solubilization with phosphatidylinositol-specific phospholipase C. *J Mol Biol 203*:821–823.

Taylor P, Jacobs NM. 1974. Interaction between bisquaternary ammonium ligands and acetylcholinesterase: Complex formation studied by fluorescence quenching. *Mol Pharmacol 10*:93-107.

Taylor P, Radić Z. 1994. The cholinesterases: From genes to proteins. *Annu Rev Pharmacol Toxicol 34*:281-320.

van den Born HKL, Radić Z, Marchot P, Taylor P, Tsigelny I. 1995. Theoretical analysis of the structure of the peptide fasciculin and its docking to acetylcholinesterase. *Protein Sci 4*:703-715.

Velan B, Kronman C, Leitner M, Grosfeld H, Flashner Y, Marcus D, Lazar A, Kerem A, Bar-Nun S, Cohen S, Shafferman A. 1992. Molecular organization of recombinant human acetylcholinesterase. In: Shafferman A, Velan B, eds. *Multidisciplinary approches to cholinesterase functions*. New York: Plenum Press. pp 39-47.

Vellom DC, Radić Z, Li Y, Pickering NA, Camp S, Taylor P. 1993. Amino acid residues controlling acetylcholinesterase and butyrylcholinesterase specificity. *Biochemistry 32*:12-17.